

Characterizing the Sensitivity to Individual Bit Flips in Client-Side Operations of the CKKS Scheme

Matías Mazzanti^{1,2}, Augusto Vega³, Esteban Mocskos^{1,2}

¹*Departamento de Computación, Facultad de Ciencias Exactas y Naturales, Universidad de Buenos Aires (Argentina)*, ²*Centro de Simulación Computacional p/Aplic Tecnológicas (CSC-CONCICET)*, ³*IBM T. J. Watson Research Center (NY, USA)*

Abstract—Homomorphic Encryption (HE) enables computation on encrypted data without decryption, making it a cornerstone of privacy-preserving computation in untrusted environments. As HE sees growing adoption in sensitive applications—such as secure machine learning and confidential data analysis—ensuring its robustness against errors becomes critical. Faults (e.g., transmission errors, hardware malfunctions, or synchronization failures) can corrupt encrypted data and compromise the integrity of HE operations.

However, the impact of soft errors (such as bit-flips) on modern HE schemes remains unexplored. Specifically, the CKKS scheme—one of the most widely used HE schemes for approximate arithmetic—lacks a systematic study of how such errors propagate across its pipeline, particularly under optimizations like the Residue Number System (RNS) and Number Theoretic Transform (NTT).

This work bridges this gap by presenting a theoretical and empirical analysis of CKKS’s fault tolerance behavior under bit-flip errors. We focus on client-side operations (encoding, encryption, decryption, and decoding) and demonstrate that while the vanilla CKKS scheme exhibits some resilience, performance optimizations like RNS and NTT exacerbate the error sensitivity of the scheme. By characterizing these failure modes, we lay the groundwork for developing HE hardware and software systems that are resilient to errors, ensuring both performance and integrity in privacy-critical applications.

Index Terms—Homomorphic encryption; resiliency; soft errors; privacy preservation

I. INTRODUCTION

The need to preserve data privacy becomes critical when processing occurs outside the user’s trusted environment, such as in public clouds or on third-party platforms. In these scenarios, protecting data not only at rest or in transit, but also during processing, is a key challenge. Homomorphic Encryption (HE) emerges as a promising technique to address this issue by enabling *computation on encrypted data* (i.e., without requiring decryption), thereby ensuring confidentiality at *all* times. For example, it allows a cloud server to calculate statistics on encrypted medical records or train a machine learning model using financial data without revealing its content. In these cases, the server performs the required operations without accessing the plaintext data, preserving its confidentiality throughout the process.

This ability to operate directly on encrypted data is not merely convenient; it is a fundamental requirement for enabling secure computation in infrastructures where full trust cannot be assumed, such as public clouds, third-party platforms, or shared devices. Without such schemes, sensitive

applications requiring delegated processing would be unfeasible from a privacy standpoint. Among the most widely used homomorphic schemes is CKKS (Cheon-Kim-Kim-Song) due to its fixed-point arithmetic support. This makes it ideal to handle real number computation in tasks such as numerical analysis, signal processing, or machine learning.

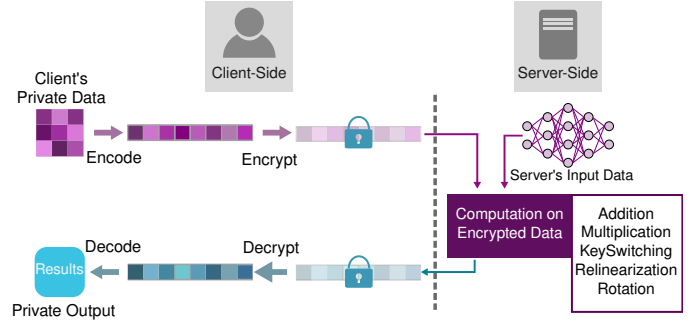


Fig. 1: Typical HE use case: a client sends encrypted data to the cloud, the cloud operates on the encrypted data and returns the results. Data and results remain encrypted all the time.

An encryption scheme should support encrypted computation of at least addition and multiplication operations in order to be considered *homomorphic*. These operations are sufficient to construct any arithmetic circuit, thereby allowing arbitrary computation without decrypting the information. In addition to these fundamental operations, some modern schemes incorporate additional primitives—such as slot rotation or complex conjugation—which, while not increasing the scheme’s expressiveness, are crucial for improving efficiency and facilitating certain computational structures, especially in applications like machine learning. HE schemes can be divided into three main categories:

- *Partial Homomorphic Encryption* (PHE) supports a single type of operation on encrypted data, either addition or multiplication. An example is The RSA (Rivest–Shamir–Adleman) cryptosystem [1], which supports multiplication of encrypted data but not addition.
- *Leveled Homomorphic Encryption* (LHE) supports both operations (addition and multiplication), but only for a limited number of steps before the accumulated noise makes correct decryption infeasible.
- *Fully Homomorphic Encryption* (FHE) enables unlimited additions and multiplications, enabling arbitrary compu-

tation on encrypted data.

As illustrated in Figure 1, the typical process for an HE scheme begins with the client encrypting data locally using a secret key before sending it to the cloud server. The server processes this data homomorphically; that is, it performs computations directly on the encrypted data. Once processing is complete, the result, which remains encrypted, is returned to the client, who is solely responsible for its decryption.

The CKKS scheme is gaining increasing interest in machine learning and data analysis applications due to its ability to perform approximate calculations on floating-point numbers. This characteristic is fundamental for efficiently handling large data volumes and training predictive models, allowing sensitive data to be processed securely without needing decryption. Despite its high computational cost, its potential in these fields is still an active area of research and development [2]–[4].

One of the most significant enhancements to the CKKS scheme is using the Residue Number System (RNS) alongside the Number Theoretic Transform (NTT). This combination has helped establish it as a standard and leads to what is known as the *full* RNS variant [5]. Throughout this paper, we will refer to this variant simply as CKKS, while the original version without these optimizations will be termed *vanilla* CKKS.

It is crucial to recognize that the CKKS scheme is vulnerable to errors caused by single bit-flips, which can compromise both computational accuracy and data integrity. Since bit-flips may occur under various conditions; therefore assessing their impact on CKKS-based applications—particularly in unreliable hardware environments—is crucial. Figure 2 illustrates a scenario in which an image from the MNIST dataset (Figure 2a) is processed through the CKKS pipeline. The effect of a single bit error introduced during the encoding phase, with the application of RNS and NTT, is depicted in Figure 2b, where a entirely distorted representation of the original image is retrieved.

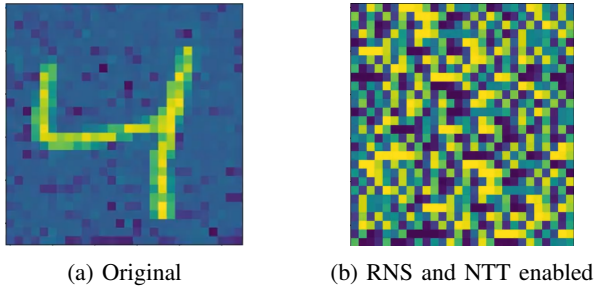


Fig. 2: Example of the impact of a single bit-flip in CKKS.

These errors can originate in hardware due to phenomena such as interference, memory failures, or even fault injection attacks [6]–[12], making bit-flip sensitivity analysis a critical aspect for the practical and reliable implementation of HE.

In this work, we conduct a comprehensive analysis of the CKKS scheme’s sensitivity to single bit errors in client-side stages, such as encoding, encryption, decryption, and decoding operations. We focus on the impact of RNS (Residue Number System) and NTT (Number Theoretic Transform) optimizations on the scheme’s resilience against these errors. To the

best of our knowledge, this paper is the first study that explores this aspect of HE. Specifically, our analysis provides a general framework aimed at enhancing the security and robustness of CKKS in diverse contexts. Our main contributions are as follows:

- We present the first comprehensive analysis of the CKKS scheme’s sensitivity to individual bit-flip errors in a typical client-side pipeline, considering configurations with and without RNS and NTT optimizations.
- We evaluate the impact of RNS and NTT optimizations on the robustness of the CKKS scheme.
- We identify specific configurations where the use of certain optimizations introduces a form of intrinsic redundancy, increasing the proportion of bits that remain correct in the presence of errors. This finding is particularly relevant for applications where fault tolerance is a fundamental requirement.
- We provide a generalized framework that can serve as a foundation for future research aimed at improving the security and resilience of CKKS against hardware failures.

Section II describes the CKKS scheme in its vanilla and full variants. Section III presents a theoretical analysis of CKKS’s robustness against bit-flip errors. Section IV details the methodology used in our experimental campaigns. The experimental analysis is developed in Section V, and finally, Section VI presents the conclusions of the work.

II. BACKGROUND AND CKKS OVERVIEW

In this section, we first introduce the core parameters of the scheme, followed by a conceptual overview alongside a simplified explanation of its key components—making the material accessible even to readers without a specialized background in cryptography.

We then delve into the mathematical foundations required for the analysis presented in Section III. Readers primarily interested in the experimental methodology may proceed directly to Section IV.

A. General Flow of the CKKS Scheme

CKKS is an approximate homomorphic encryption scheme designed to enable computations on encrypted data while providing explicit control over approximation error. It operates over a polynomial ring of degree N based on the Ring Learning With Errors (RLWE) problem, a lattice-based problem that ensures security through the controlled injection of noise into ciphertexts.

CKKS supports the encrypted processing of vectors of real or complex numbers, without ever revealing the original data.

Figure 1 presents the FHE’s process consisting of five main stages:

- 1) **Key Generation:** The secret key and public key are generated as degree- N polynomials, created through random sampling and error injection.
- 2) **Encoding:** The input vector is transformed using a specialized inverse Fast Fourier Transform (IFFT) into

a degree- N polynomial, constructed such that its evaluations at certain roots of unity approximately reproduce the original values. The resulting polynomial's coefficients are then scaled by Δ and rounded to integers, producing the *plaintext*. Formally, given a polynomial P and a vector $z \in \mathbb{R}^N$, the following relation holds:

$$z = (P(\xi), P(\xi^3), \dots, P(\xi^{2N-1})).$$

A specialized version of the FFT, adapted to the ring $\mathbb{Z}_q[X]/(X^N + 1)$, is used to preserve the algebraic structure of the scheme and enable various optimizations.

- 3) **Encryption:** Given the plaintext, two encrypted polynomials (c_0, c_1) are generated using the public (or secret) key and by adding a small amount of noise. The result $c = (c_0, c_1)$ is referred to as the **ciphertext**.
- 4) **Computation:** Homomorphic operations are performed directly on the ciphertexts, including addition, multiplication, rotations, and other transformations compatible with the scheme.
- 5) **Decryption and Decoding:** The ciphertext is multiplied by the secret key and summed. The result is then divided by Δ , and a specialized FFT is applied to recover an approximation of the original input vector.

Since the security of CKKS relies on the computational hardness of the RLWE problem, each encryption inherently introduces noise. Although it is small at the beginning, it accumulates during homomorphic operations. Each operation increases the noise level in the ciphertext, with homomorphic multiplication contributing the most to this growth.

For this reason, the number of successive multiplications is often used as an indirect estimate of the accumulated error in a ciphertext. If this growth is not properly managed—e.g., through techniques such as bootstrapping—the error can exceed tolerable limits, resulting in incorrect outputs during decryption and decoding.

B. Parameters controlling CKKS

CKKS operates over a polynomial ring defined as:

$$\mathcal{R}_q = \mathbb{Z}_q[X]/(X^N + 1),$$

where \mathbb{Z}_q denotes the integers modulo q , that is, the integer values between 0 and $q - 1$ (addition and multiplication are performed modulo q), $\mathbb{Z}_q[X]$ denotes the polynomials with coefficients in \mathbb{Z}_q , and $/(X^N + 1)$ indicates that polynomials are considered modulo $X^N + 1$.

This ring imposes a negacyclic structure that enables, after encoding, the efficient representation of vectors of complex numbers. In CKKS, data is encoded as a polynomial that, when evaluated at specific values, yields each of the encoded data points. In particular, the degree N must be a power of two and serves two critical purposes: it determines the maximum number of complex values that can be encoded simultaneously ($N/2$), and it is essential for maintaining the security of the scheme.

The original (i.e., vanilla) version of the CKKS scheme uses the following core parameters, which are selected to achieve

the desired security level, maintain tolerable error growth, and minimize computational cost:

- N is the ring degree, typically in the range 2×10^{12} to 2×10^{16} , and it determines both the dimension of the encoding space and the computational cost.
- q_0 is the initial modulus—a single large integer (typically up to 60 bits)—that largely defines the target precision.
- Δ is the scaling factor, a constant used to amplify real values before encoding to preserve floating-point precision.
- L is the multiplicative depth, that is, the number of homomorphic multiplications that can be performed before accumulated noise degrades precision.

The total modulus of the scheme, denoted Q , and the size of the coefficients in the encoding and encryption polynomials are defined differently depending on the CKKS variant used. In the vanilla version, Q is given by:

$$Q = \Delta^L \cdot q_0,$$

In CKKS, each multiplication between ciphertexts increases both the error and the magnitude of the encoded values. To control this growth and preserve precision, an operation called *rescaling* is applied. Rescaling reduces the scale of the encoded values and also decreases the active modulus, which in turn limits the number of consecutive multiplications (with rescaling) that can be performed. This limit is known as the **multiplicative depth** of the scheme. The parameter Δ is applied L times—once for each multiplicative level supported by the modulus hierarchy.

1) **CKKS full RNS variant:** The **Residue Number System** (RNS) is an alternative representation of integers that expresses a number through its residues modulo several small, pairwise coprime integers. This encoding allows arithmetic operations—such as addition and multiplication—to be performed independently and in parallel on each modulus, reducing computational complexity and significantly improving efficiency. These properties make RNS particularly well-suited for high-performance contexts such as homomorphic encryption.

The use of the **Chinese Remainder Theorem** (CRT) is essential in RNS, as it ensures that each set of residues uniquely corresponds to a single integer within a defined range. Moreover, CRT provides an efficient procedure to reconstruct the original integer from its residue representation.

In the RNS-optimized variant of the CKKS scheme, all polynomials involved (i.e., messages, keys, and ciphertexts) are represented as multiple polynomials of the same degree, one for each residue modulo in the RNS base. Additionally, each of these polynomials is transformed using the Number Theoretic Transform (NTT)—a modular analogue of the Fast Fourier Transform (FFT). NTT accelerates polynomial multiplication, which is one of the most computationally intensive operations in the scheme.

These optimizations—RNS and NTT—do not alter the semantics of the encryption scheme but do change its internal implementation. In particular, they have implications for error propagation and sensitivity, topics that will be analyzed in detail in Section III.

In this variant, the total modulus of the scheme is expressed as:

$$Q = \prod_{i=0}^{L-1} q_i, \quad (1)$$

where q_0 is the initial modulus and q_1, \dots, q_L are additional moduli that in general are selected by the scheme, all of similar bit length. It is worth noting that some libraries provide manual control over the bit-length of these q_i moduli; the implementations employed in this work automatically configure these parameters according to the bit length specified for q_0 .

C. CKKS' Insights

The CKKS scheme accepts as input a vector of up to $N/2$ floating-point elements, i.e., $\in \mathbb{C}^{N/2}$. This input is mapped into the polynomial ring $\mathbb{Z}[X]/(X^N + 1)$ through a process known as encoding, producing a plaintext polynomial m . Here, $\mathbb{Z}[X]$ denotes the ring of polynomials with integer coefficients, and $\mathbb{Z}[X]/(X^N + 1)$ is the quotient ring where polynomials are reduced modulo $X^N + 1$. This implies working with polynomials of degree at most $N - 1$ under negative (or negacyclic) convolution. In this context, polynomial reduction is performed via the substitution $X^N = -1$, ensuring that results remain within the allowed polynomial space of degree less than N .

The resulting plaintext is then encrypted using either the public or secret key, following the RLWE problem, where a small amount of noise is intentionally injected for security. The ring $\mathbb{Z}[X]/(X^N + 1)$ is preferred in RLWE-based schemes due to its stronger security properties compared to $\mathbb{Z}[X]/(X^N - 1)$, where the convolution is cyclic and considered more vulnerable to attacks.

a) Precision: To better understand the parameter selection in CKKS, it is helpful to clarify the concept of precision. In the case of OpenFHE with real-valued inputs only, the scaling parameter Δ determines how many bits are used to encode the fractional part of the input values, and the difference between the initial modulus q_0 and Δ indicates the number of bits allocated to the integer part.

For example, using $q_0 = 60$ bits and $\Delta = 50$ bits allows the encrypted representation of real numbers with approximately 10 bits of precision for the integer part and 50 bits for the fractional part.

b) Keys: Encryption in the CKKS scheme requires either a secret key sk or a public key pk . The secret key is generated by sampling a vector s of length N generally from a ternary distribution with Hamming weight h , and then setting $sk = (1, s)$.

The public key is constructed by sampling a_0 from \mathbb{Z}_Q , i.e., from the set of positive integers less than the modulus Q , and an error term e_0 from a discrete Gaussian distribution with standard deviation $\sigma = 3.2$. The public key is then defined as:

$$pk = ([-a_0s + e_0]_Q, a_0) = (p_0, p_1)$$

where the notation $[\dots]_Q$ denotes reduction modulo Q .

c) Encoding: The key idea behind encoding in CKKS is to transform the input vector into a polynomial. Different libraries implementing CKKS vary in how they perform this transformation using IFFT/FFT-based methods. In all cases, the standard cyclic transform must be adapted to a negacyclic version to ensure operations remain within the ring $\mathbb{Z}_q[X]/(X^N + 1)$ used by the scheme.

The transforms employed by HEAAN 1.0 and OpenFHE 1.3.0 are negacyclic and include scheme-specific optimizations, commonly referred to as specialized FFT/IFFT. These versions incorporate several improvements originally proposed by Bernstein [13], [14]. One of their main advantages is that they allow the transform to be applied directly to vectors of size $\leq N/2$, without expanding them to size N , which significantly reduces computational cost.

Given a real-valued input vector of size $n \leq N/2$, the encoding process begins by padding the vector with zeros to reach the next power of two, denoted n' . A specialized inverse FFT is then applied, producing a complex vector of length n' . From this, a polynomial of degree $N - 1$ is constructed.

First, the gap parameters $= \frac{N/2}{n'}$ are computed, and the lower half of the polynomial (coefficients of degree 0 to $N/2 - 1$) is filled with the real parts of the transformed vector, with assignments spaced at intervals of size *gap*. The upper half does the same, but using the imaginary part of the transformed vector. Unassigned coefficients are set to zero.

Finally, as is illustrated in Fig. 3, each coefficient is multiplied by Δ , and then rounded to the nearest integer using the coordinate-wise randomized rounding method described in [15].

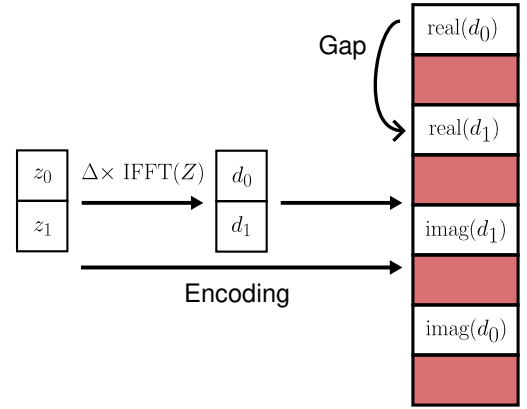


Fig. 3: Encoding scheme in CKKS using HEAAN/OpenFHE. The example shows an input vector with $n = 2$ values, represented in a polynomial ring of size $N = 8$, where the gap between consecutive coefficients is 2.

d) Encryption: The encryption of a plaintext m using the secret key $sk = (1, s)$ and modulus Q is given by:

$$c_{sk} = ([m + a \times s + e]_Q, [-a]_Q) = (c_0, c_1) \quad (2)$$

where a is a polynomial sampled from a uniform distribution, e is a noise term sampled from a discrete Gaussian distribution, and the notation $[\dots]_Q$ denotes reduction modulo Q .

An alternative procedure is to encrypt by using the public key, $pk = (p_0, p_1)$. In this case, encryption is defined as:

$$c_{pk} = ([m + p_0 \times v + e_1]_Q, [p_1 \times v + e_2]_Q) = (c_0, c_1) \quad (3)$$

where v is an ephemeral (one-time) polynomial sampled from a ternary distribution, and e_1, e_2 are error terms sampled similarly to e in the previous procedure.

e) Decryption: Decryption in both cases (secret key and public key encryption) uses the secret key $sk = (1, s)$ and the encrypted text (c_0, c_1) as follows:

$$m' = [c_0 + c_1 \times s]_Q \quad (4)$$

f) Decoding: To decode a plaintext polynomial m with N coefficients, one must reconstruct a complex-valued vector of n' elements by reversing the encoding process illustrated in Fig. 3. The i -th element ($i \leq N/2$) of the resulting vector is formed by using the real part of the i -th coefficient of the plaintext, and the imaginary part from the coefficient at position $i + N/2$.

This complex vector is then divided by Δ , and a specialized FFT is applied to recover the approximate original input.

Due to rounding effects during encoding and decoding, the final result may contain small approximation errors. Corollary 3 in [16] shows that the worst-case distance between the input vector z and the output vector z' (after encoding and decoding) at each position is approximately: $N/(\pi \times \Delta)$.

With a sufficiently large Δ , this difference becomes negligible. Given that a typical ring size N ranges from 2×10^{12} to 2×10^{16} , using a scaling factor on the order of 2^{20} is enough to ensure a reasonable approximation error. In our case, since we use a smaller N for practical reasons, the approximation error is even smaller and can be considered negligible.

g) Security Against Secret Key Attacks: To defend against secret key recovery attacks, `OpenFHE` performs additional operations before applying the specialized FFT during the decoding process. Specifically, a Gaussian error is injected before this step, with its standard deviation determined by the vector being decoded. This mechanism is critical: in our bit-flip experiments—when security analysis is not disabled—the software throws an exception during this stage, resulting in premature termination of execution.

This behavior demonstrates the role of these protective measures in preventing potential side-channel or fault-injection attacks that could compromise the secret key.

D. RNS and NTT Optimizations

In the full RNS/NTT variant of CKKS [5], the Residue Number System (RNS) is used to split large polynomial coefficients into multiple smaller values, enabling improvements in throughput of up to an order of magnitude. This approach enables arithmetic in \mathbb{Z}_Q to be performed using standard machine word sizes by working with small moduli that simplify computation.

The magnitude of the modulus Q can range from hundreds to thousands of bits, depending on the use case. However, modern computing systems typically operate with word sizes of 64 bits or less, making direct operations on such large

coefficients impractical. To address this, polynomials (keys, plaintexts, ciphertexts) are represented using an equivalent decomposition in the RNS form. Each coefficient is represented modulo a small prime q_i , to generate Q like Eq. 1

This decomposition enables addition and multiplication in \mathbb{Z}_Q using standard machine word operations. All other parameters, as well as the encoding and decoding procedures, remain consistent with the vanilla CKKS variant.

Polynomial multiplications are performed efficiently using the Number Theoretic Transform (NTT), which reduces the computational complexity of the operation from $\mathcal{O}(n^2)$ to $\mathcal{O}(n \log n)$. Addition of polynomials and multiplication by a scalar are both $\mathcal{O}(n)$ operations in both the coefficient and evaluation (NTT) representations.

By default, the CKKS scheme assumes that polynomials are represented in the NTT domain (evaluation representation). When certain operations require polynomials in coefficient form, an inverse NTT (iNTT) is applied to transform ciphertexts from the evaluation domain back to the coefficient domain. However, within the scope of this work, as all computations are performed on the client side, this change of representation does not occur.

The procedures for encoding, encryption, decryption, and decoding remain virtually unchanged, except that all operations are now performed using the RNS and NTT representations.

III. ERROR RESILIENCE ANALYSIS

This section presents a theoretical analysis of the error induced by a single bit-flip at different stages of the CKKS scheme. We address both the vanilla and the full RNS variant versions. Our aim is:

- Deriving analytical bounds in the case without RNS or NTT.
- Identifying the most sensitive coefficients.
- Providing an intuitive description of error behavior in practical implementations.

Although a closed-form analytical bound can not be derived for the full RNS variant due to the complexity of modular representations, a qualitative analysis of the observed patterns is provided.

A. Error Model for a Single Bit-Flip

We adopt a single bit-flip model, where a single bit is altered. In practice, such faults may be caused by electromagnetic interference, hardware failures, or cosmic rays [6], [7], [9], [11], [17], [18].

Let p be the original value of a coefficient, either in a plaintext polynomial \mathbf{m} or in one of the ciphertext polynomials (c_0, c_1) . We denote this generic polynomial as \mathbf{p} . Let's p'_j be the result of flipping a bit j of p , then the resulting error is:

$$e_j = p'_j - p \quad (5)$$

We model this fault as an error vector $\mathbf{e}_{i,j} \in \mathbb{R}^N$ whose only non-zero component corresponds to bit j of coefficient i :

$$\mathbf{e}_{i,j} = (0, \dots, 0, e_j, 0, \dots, 0) \quad (6)$$

This model enables us to track how a single bit-flip propagates through the cryptographic pipeline.

B. CKKS Encoding via DFT

As discussed in Section II, one of the key components of encoding and decoding in CKKS is FFT. Although CKKS uses a specialized inverse FFT for computational efficiency, this transformation is typically implemented using optimized algorithms that obscure its underlying linear structure.

Instead, we rely on the negacyclic Discrete Fourier Transform (DFT), an algebraically equivalent transformation explicitly expressed as matrix multiplication. This formulation allows us to:

- 1) Directly represent how errors propagate through the encoding process.
- 2) Analyze the isolated effect of a perturbation in a single coefficient.
- 3) Derive analytical bounds on the magnitude of the error without dealing with the internal optimizations of FFT implementations.

While this choice sacrifices performance, it offers significant pedagogical advantages, allowing for an intuitive understanding of how bit-flip errors are amplified or distributed during the encoding stage.

1) *Encoding via Negacyclic DFT*: Let $M = 2N$ and $\xi = e^{-2\pi i/M}$. To construct a negacyclic Discrete Fourier Transform (DFT), we evaluate it at the odd powers of the roots of the cyclotomic polynomial $\Phi_M(X) = X^N + 1$; that is, at $\xi^1, \xi^3, \xi^5, \dots, \xi^{2N-1}$. We define the **Vandermonde matrix** where each column corresponds to a different power of these roots of unity:

$$W = \begin{pmatrix} \xi^{1 \cdot 0} & \xi^{1 \cdot 1} & \dots & \xi^{1 \cdot (N-1)} \\ \xi^{3 \cdot 0} & \xi^{3 \cdot 1} & \dots & \xi^{3 \cdot (N-1)} \\ \vdots & \vdots & \ddots & \vdots \\ \xi^{(2N-1) \cdot 0} & \xi^{(2N-1) \cdot 1} & \dots & \xi^{(2N-1) \cdot (N-1)} \end{pmatrix} \quad (7)$$

and we denote its inverse as W^{-1} , which is required for the encoding process. Due to the properties of this matrix, its inverse is simply the conjugate transpose (Hermitian transpose) normalized by N :

$$W^{-1} = \frac{1}{N} W^\dagger$$

To use the DFT and its inverse for encoding to obtain results equivalent to those produced by implementations such as HEAAN and OpenFHE, some preprocessing is required: the input vector must be resized to length N and reordered to satisfy the requirements of those systems. However, these adjustments do not affect the behavior of the error model under analysis and are omitted for simplicity.

In general, for an input vector of $n \leq N/2$ elements, it is first zero-padded to length $N/2$, and then mirrored with its complex conjugate to reach a total length of N . Once the input vector $\mathbf{z} \in \mathbb{R}^N$ is prepared and reordered, the encoding proceeds as follows:

$$\begin{aligned} \text{Encode}(\mathbf{z}) &= \text{Round}(W^{-1}(\Delta \mathbf{z})) \\ &= \text{Round}(\Delta \cdot W^{-1} \mathbf{z}) = \mathbf{m} \in \mathbb{Z}^N, \end{aligned} \quad (8)$$

where Δ is the already defined scaling factor. Due to the Hermitian symmetry of W and W^{-1} , and the conjugate extension of the input, the result of $W^{-1} \mathbf{z}$ lies entirely in the real subspace.

To recover an approximation of the original input \mathbf{z} from \mathbf{m} , decoding is performed as:

$$\text{Decode}(\mathbf{m}) = \mathbf{z}' = W(\mathbf{m}/\Delta) \quad (9)$$

Finally, the output undergoes the same reordering process as in encoding, and the n components of \mathbf{z}' are extracted. Since the DFT output is complex-valued while OpenFHE supports only real-valued encryption, the real part is extracted to obtain the final approximation of \mathbf{z} .

C. Theoretical Estimation of Encoding Error in Vanilla CKKS

This section focuses on the impact of single-bit errors during the encoding phase of the CKKS scheme.

Let us consider the case in which an error $\mathbf{e}_{i,j}$ is introduced by flipping a single bit in the coefficient i of the plaintext vector \mathbf{m} , specifically at the j -th bit position. The resulting perturbed plaintext is $\mathbf{m}' = \mathbf{m} + \mathbf{e}_{i,j}$, and decoding proceeds as in Eq. 9:

$$\begin{aligned} \mathbf{z}'' &= W \times \frac{\mathbf{m}'}{\Delta} = W \times \frac{\mathbf{m} + \mathbf{e}_{i,j}}{\Delta} \\ &= W \times \frac{\mathbf{m}}{\Delta} + W \times \frac{\mathbf{e}_{i,j}}{\Delta} \\ &= \mathbf{z}' + W \times \frac{\mathbf{e}_{i,j}}{\Delta} \end{aligned}$$

Since a single bit-flip affects only one coefficient, the resulting error is localized. The difference between the decoded vectors \mathbf{z}' and \mathbf{z}'' is given by:

$$\|\mathbf{z}' - \mathbf{z}''\| \propto \|W \times \mathbf{e}_{i,j}/\Delta\| \quad (10)$$

1) *Bit-Flip Injection during Encoding*: To better understand the analytical expression of the error in Eq. (10), we simulate flipping each bit in the plaintext coefficients. Let $j \in \{0, \dots, 63\}$ denotes the bit position in a 64-bit unsigned integer. For each iteration, we flip the j -th bit of a coefficient, introducing an error with integer magnitude $e_j = 2^j$. This represents the maximum jump in value induced by flipping bit j in a coefficient, which is stored as an unsigned integer—as in the case of plaintext coefficients.

We repeat this process for all coefficients, grouping the results into $N = 4$ blocks of 64 iterations each, and use $\Delta = 2^{50}$. Let \mathbf{z}' be the decoded vector without errors, and \mathbf{z}'' the result after applying the bit-flip and decoding. Using Eq. (10), we define:

$$L_2(i, j) = \| \text{Real}(W \times \mathbf{e}_{i,j}/\Delta) \|_2 \quad (11)$$

where $\mathbf{e}_{i,j}$ is a zero vector of length N with value e_j at position i .

We also take the real part of the vector before computing the L2 norm, to simulate the encoding of real-valued data, as in OpenFHE, in contrast to HEAAN, which allows complex inputs. This step is important not only to maintain consistency with the backend used in later sections, but also because it exposes a specific behavior that would otherwise not manifest when keeping the complex part.

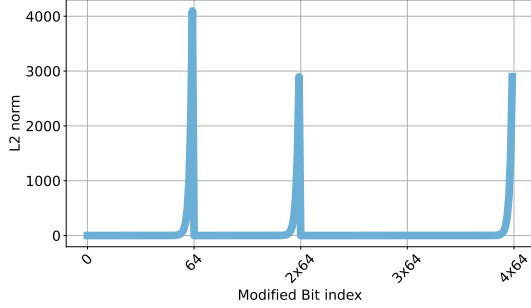


Fig. 4: L_2 norm of the error after a single bit-flip in the plaintext during encoding. The horizontal axis shows the bit-flip position. Ring dimension $N = 4$; scaling factor $\Delta = 2^{50}$.

Figure 4 shows the values of $L_2(i, j)$ as a function of the bit-flip position. $L_2(i, j)$ grows exponentially with j for each coefficient i , consistent with the 2^j dependency. An exception appears at $i = N/2 = 2$, where the norm remains zero. This occurs because, in the DFT, the coefficient at index $N/2$ contributes only imaginary components, which vanish when taking the real part of the transform.

2) *Effect of the Scaling Factor on Bit-Flip Error:* To explore how the scaling factor Δ affects the magnitude of bit-flip errors, we repeat the previous experiment using different values of $\Delta \in \{2^{20}, 2^{40}, 2^{50}\}$. For each case, we plot $L_2(i, j)$ using a semi-logarithmic scale on the y -axis for easier comparison.

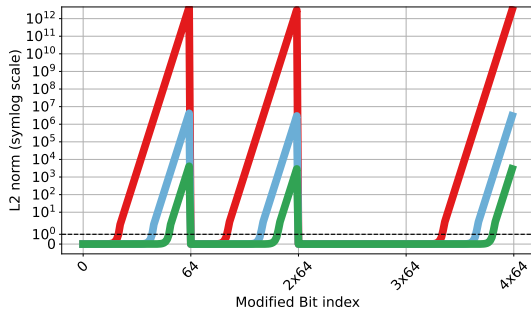


Fig. 5: L_2 norm of the error after a single bit-flip in the plaintext during encoding, for various scaling factors Δ . The horizontal axis indicates the bit position j ; the vertical axis is on a semi-log scale. Ring dimension: $N = 4$.

As shown in Fig. 5, increasing Δ significantly reduces the error magnitude and increases the number of *resilient* bits. This occurs because the impact of errors becomes noticeable only when the flipped bit corresponds to or exceeds the magnitude of Δ . In other words, the larger the scaling factor, the more

initial bits remain unaffected, yielding smaller error norms and higher bit-level fault tolerance.

This empirical observation is confirmed analytically by equation 11, which shows that the error is inversely proportional to the scaling factor. When an error $e_{i,j}$ is divided by Δ , noise components with magnitudes smaller than the bit precision of Δ are effectively suppressed in the final result. This mathematical relationship explains why larger scaling factors provide enhanced fault resilience: they act as a natural filter that attenuates the impact of small-magnitude bit-flips on the decoded output.

However, this resilience comes at the cost of reduced fractional precision in the encoded message (see Section II). The selection of Δ therefore requires careful consideration, balancing the competing demands of fault resilience and computational accuracy.

D. Theoretical Estimation of Error during Encryption using Vanilla CKKS

This section analyzes three scenarios involving a single bit-flip in vanilla CKKS:

- 1) A bit-flip in the plaintext (before encryption).
- 2) A bit-flip in the ciphertext (in one of the ciphertext polynomials).
- 3) A bit-flip in the plaintext (before decoding).

Under public-key encryption, a plaintext vector \mathbf{m} is encoded into a polynomial $\mathbf{m}(X)$, encrypted as in Eq. 3, and decrypted using Eq. 4.

1) *Bit-Flip in the Plaintext Before Encryption:* Suppose a bit-flip introduces an error $e_{i,j}$ in the i -th coefficient at bit position j , so the plaintext becomes:

$$\mathbf{m}' = \mathbf{m} + \mathbf{e}_{i,j}, \quad \mathbf{e}_{i,j} = e_j X^{i-1} \quad (12)$$

Encrypting \mathbf{m}' using the public key (as in Eq. 3) yields:

$$\begin{aligned} ct' &= ([\mathbf{m}' + p_0 v + e_1]_Q, [p_1 v + e_2]_Q) \\ &= ([\mathbf{m} + e_j X^{i-1} + p_0 v + e_1]_Q, c_1) = (c'_0, c_1). \end{aligned} \quad (13)$$

The error affects only the ciphertext component c'_0 in the coefficient i , with a maximum magnitude $|e| \leq Q/2$ due to modular arithmetic. Upon decryption (using Eq. 4):

$$\mathbf{m}'' = [c'_0 + c_1 s]_Q = \mathbf{m} + e_j X^{i-1} + (e_1 + e_2 s) \quad (14)$$

However, the error magnitude grows exponentially with the flipped bit position, as each bit represents a successive power of 2 in the binary representation. Consequently, an exhaustive bit-flip analysis across all coefficient positions, with L2 norm computation for each perturbation, yields the exponential error scaling pattern illustrated in Fig. 4 (Section III-C). The bit-flip impact remains localized to the position i and scales linearly with e_j .

The error induced by the bit-flip affects only the ciphertext component c'_0 in coefficient i , with a maximum magnitude $|e| \leq Q/2$ due to modular arithmetic. Decoding this plaintext will therefore produce an error consistent with that discussed in Section III-C.

2) *Bit-Flip in the Ciphertext:* If the bit-flip occurs in the ciphertext, two sub-cases arise:

a) *Flip in c_0* : For a perturbed ciphertext $ct' = (c_0 + e_j X^{i-1}, c_1)$, the behavior mirrors the previous plaintext case: the error remains localized in coefficient i and results in a decoding error proportional to e_j .

b) *Flip in c_1* : For a perturbed ciphertext $ct' = (c_0, c_1 + e_j X^{i-1})$, decryption proceeds as:

$$\begin{aligned} \mathbf{m}'' &= [c_0 + (c_1 + e_j X^{i-1})s]_Q \\ &= [(c_0 + c_1 s) + (e_j X^{i-1} s)]_Q \\ &= [(\mathbf{m} + e_1 + e_2 s) + (e_j X^{i-1} s)]_Q \end{aligned}$$

where $e_j X^{i-1} s$ involves polynomial multiplication. Thus, the error spreads across all N coefficients. Since the secret key s has small coefficients (much less than q_0), each coefficient in the result incurs an error of magnitude proportional to e_j , but this error is now distributed. The maximum magnitude is bounded by $|e_j| \cdot \|s\|_\infty$.

3) *Bit-Flip in the Plaintext Before Decoding*: If a bit-flip is introduced in the coefficient i of a plaintext \mathbf{m} , after decryption but before decoding, the effect is analogous to the case analyzed in Section III-C. This follows directly since the plaintext being decoded is equivalent to:

$$\mathbf{m}' = \mathbf{m} + e_j X^{i-1} \quad (15)$$

which is the same structure previously analyzed.

E. Theoretical Estimation of Error in RNS

CKKS typically uses a Residue Number System (RNS) representation for the modulus $Q = \prod_{k=0}^{L-1} q_k$, where L determines the number of available levels (i.e., number of supported homomorphic operations).

Each coefficient $p \in \mathbb{Z}_Q$ is represented by its residues:

$$r_k = p \bmod q_k \quad \text{for } k = 0, \dots, L$$

When applied to all coefficients of a polynomial (from an encoded message or ciphertext), this yields L **residue polynomials**, commonly referred to as **limbs**. Reconstruction via the Chinese Remainder Theorem (CRT), as shown in Mohan [19, Chapter 5], is:

$$p = \left(\sum_{k=1}^L r_k \left[\left(\frac{1}{Q_k} \right) \bmod q_k \right] Q_k \right) \bmod Q \quad (16)$$

where

$$Q_k = Q/q_k$$

and $\frac{1}{Q_k}$ are the multiplicative inverse of Q_k .

A bit-flip on the j bit affecting the k -th residue changes it to $r'_k = r_k + e_{k,j}$, which introduces an error into the reconstructed value:

$$p' = p + e_{k,j} Q_k \left[\left(\frac{1}{Q_k} \right) \bmod q_k \right] \pmod{Q} \quad (17)$$

This error can be as large as Q_k , potentially spanning hundreds or thousands of bits, even though the bit-flip affected only one bit in a single residue.

F. Theoretical Estimation of Error in NTT

To accelerate encoding and decoding operations, CKKS uses the Negacyclic Number Theoretic Transform (NTT) over the ring $\mathbb{Z}_q[X]/(X^N + 1)$. Let $\psi \in \mathbb{Z}_q$ be a primitive $2N$ -th root of unity satisfying:

$$\psi^2 \equiv \xi, \quad \psi^N \equiv -1 \pmod{q},$$

where ξ is a primitive N -th root of unity. The NTT matrix is defined as:

$$W_{NTT} = \begin{pmatrix} \psi^{2(0 \times 0) \cdot 0} & \psi^{2(0 \times 1) \cdot 1} & \dots & \psi^{2(0 \times N-1) \cdot N-1} \\ \psi^{2(1 \times 0) \cdot 0} & \psi^{2(1 \times 1) \cdot 1} & \dots & \psi^{2(1 \times N-1) \cdot N-1} \\ \psi^{2(2 \times 0) \cdot 0} & \psi^{2(2 \times 1) \cdot 1} & \dots & \psi^{2(2 \times N-1) \cdot N-1} \\ \vdots & \vdots & \ddots & \vdots \\ \psi^{2(N-1 \times 0) \cdot 0} & \psi^{2(N-1 \times 1) \cdot 1} & \dots & \psi^{2(N-1 \times N-1) \cdot N-1} \end{pmatrix}$$

We denote its inverse as W_{NTT}^{-1} . When a single bit-flip occurs at bit position j within coefficient i , the induced perturbation after NTT transformation becomes:

$$\mathbf{m}' - \mathbf{m} = W_{NTT} \mathbf{e}_{i,j}.$$

Therefore, the L_2 norm of the error is:

$$\|\mathbf{m}' - \mathbf{m}\|_2 = \|W_{NTT} \mathbf{e}_{i,j}\|_2.$$

This behavior parallels that of the Discrete Fourier Transform (DFT), except that the NTT operates over \mathbb{Z}_q with moduli q typically of 30 bit to 60 bit. The twiddle factors, being roots of unity modulo q , can amplify errors during the transformation, thereby increasing the error.

Figure 6 shows the values of $L_2(i, j)$ for $N = 4$ and 64-bit coefficients in the NTT case. The horizontal axis indicates the bit-flip position $i \cdot 64 + j$, and the vertical axis shows $L_2(i, j)$ on a logarithmic scale.

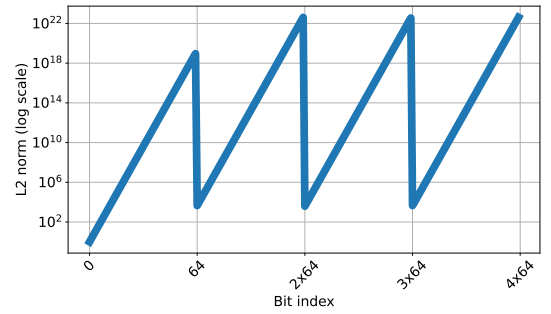


Fig. 6: L_2 norm of the error after a single bit-flip in the plaintext during encoding. The horizontal axis shows the modified bit position $i \cdot 64 + j$; the vertical axis shows the $L_2(i, j)$ norm on a logarithmic scale. Ring dimension: $N = 4$.

As the Fig. 6 shows, even the flips in the least significant bits cause the norm to exceed four orders of magnitude—producing errors large enough to make correct decoding practically impossible, as will be further illustrated in Section V.

G. Summary

The following points summarize the theoretical impact of a single bit-flip at different stages of the CKKS encryption pipeline, both in its vanilla and optimized implementations:

- **Bit-flip in the plaintext before encryption:** the error remains localized in a single coefficient where the bit-flip occurred, with a magnitude proportional to $e_j = 2^j$, depending on the flipped bit's position j .
- **Bit-flip in the ciphertext (c_0):** identical to the plaintext case—the error remains localized after decryption, with magnitude again proportional to the bit position j .
- **Bit-flip in the ciphertext (c_1):** the error is multiplied by the secret key s , becoming distributed across all N coefficients; its maximum magnitude is $\mathcal{O}(e_j \|s\|_\infty)$.
- **Bit-flip in the plaintext before decoding:** behaves like a localized error in a single coefficient of the encoded polynomial—effectively equivalent to the encoding case, plus minor encryption noise.
- **RNS:** a bit-flip in a single *limb* (residue) can result in a reconstruction error of order $\mathcal{O}(Q_k)$, where $Q_k = Q/q_k$ is typically a large value.
- **Negacyclic NTT:** a bit-flip before or after the NTT produces an error proportional to $W_{NTT} \mathbf{e}_{i,j}$, spreading across all coefficients. Entries of W_{NTT} are bound by modulus q , which typically ranges from 30 bit to 60 bit, thus potentially amplifying the error significantly.

IV. EXPERIMENTAL DESIGN

This section describes the experimental design used to quantify the resilience of the CKKS HE scheme under single bit-flip fault injections.

A. Scheme Definition and Operational Assumptions

We consider four experimental configurations using CKKS:

- **Vanilla mode:** All low-level performance optimizations are disabled; arithmetic occurs in a single large modulus in coefficient space (single limb, no NTT domain representation).
- **RNS-only mode:** Residue Number System (RNS) decomposition is enabled (multi-limb representation), but the NTT (evaluation-domain transform) is forcibly bypassed.
- **NTT-only mode:** The Number Theoretic Transform (NTT) is enabled to accelerate polynomial multiplication / convolution, while RNS decomposition is disabled (single-limb modulus).
- **RNS+NTT mode:** Fully optimized configuration (default in OpenFHE) with both RNS decomposition and NTT-based evaluation.

This setup allows us to isolate the individual and combined effects of RNS and NTT optimizations on fault propagation and resilience, while maintaining compatibility with standard security parameters.

In preliminary tests, we observed that both the *NTT-only* and *RNS+NTT* configurations lead to widespread error amplification even from single-bit faults, consistently with our

theoretical analysis (Sec. III). As a result, we focus our analysis on the *Vanilla* and *RNS-only* modes, where more nuanced fault behavior can be observed and meaningfully characterized.

B. Fault / Error Injection Model

As in our theoretical analysis (Sec. III-A), we assume a transient single-bit fault model, motivated by soft errors such as radiation-induced bit flips in processor registers or memory buffers. Specifically, we inject a single bit-flip in one coefficient of the output of a given operation (e.g., Encode, Encrypt, Decrypt, or Decode) during each execution. In the case of Encode and Decode, we inject the fault into the plaintext representation; for Encrypt and Decrypt, we inject it into the ciphertext. This models a fault affecting the destination register or output memory of these functions, without modifying the inputs or intermediate computations.

The fault is injected at a single stage per experiment, directly on the polynomial representation (plaintext or ciphertext), simulating a post-operation corruption that propagates through subsequent stages of the computation.

C. Implementations and Instrumentation

1) *CKKS baseline:* We use two different CKKS implementations to cover both the vanilla and optimized variants of the scheme:

- **HEAAN 1.0:** a vanilla implementation without RNS or NTT, using arbitrary-precision coefficients managed by the NTL library (a C++ library for number theory and arbitrary-precision arithmetic).
- **OpenFHE 1.3.0:** a modular implementation with native support for RNS and NTT, using 64-bit internal coefficients (`uint64`).

Although more recent versions of HEAAN include RNS and NTT optimizations, version 1.0 allows a cleaner comparison to a vanilla CKKS. Conversely, OpenFHE represents the optimized variant, due to its widespread use in the field of homomorphic encryption [20] and its active support for high-performance execution environments.

We minimally modify both libraries to gain complete control over the selection of pseudo-random number generator (PRNG) seeds. This ensures strict reproducibility of experiments and allows precise isolation of the effects caused by each bit-flip.

In the case of HEAAN 1.0, we have these additional implementation details:

- The bit-length of each plaintext coefficient is not fixed in advance; it depends on internal combinations of q_0 and Δ , and may vary depending on the PRNG seed used by the scheme.
- The ciphertext bit-length is of length q_0 .
- Due to NTL implementation, bits larger than the Q of the coefficient are ignored in internal operations, which limits the scope of bit-level analysis.

OpenFHE has the following implementation details:

- Uses 64-bit integer coefficients (`uint64_t`) without arbitrary-precision arithmetic.
- The user can configure the initial modulus q_0 . This parameter determines the starting bit-level precision of the scheme. The subsequent moduli q_i are automatically selected to match the bit length of q_0 , ensuring uniform precision across levels.
- The total number of moduli depends on the required multiplicative depth of the computation.
- Public APIs for accessing and modifying coefficients at each pipeline stage (i.e., encoding, encryption, etc.).
- Enables injection of fixed-length bit-flips (up to 64 bits) at controlled and reproducible positions.
- Supports 128-bit arithmetic, which—though not used in this work—offers a pathway for future experiments.

2) Using *OpenFHE* as Vanilla CKKS implementation:

OpenFHE is significantly more computationally efficient than *HEAAN*. However, it does not natively offer a mechanism to disable RNS and NTT optimizations. To address this, we devised a procedure to emulate a vanilla CKKS scheme within *OpenFHE* by explicitly bypassing both RNS and NTT optimizations, despite their built-in support in the library:

- **RNS:** We enforced a single-limb representation, which is feasible for depth-zero operations (i.e., no ciphertext multiplications). Additionally, automatic rescaling was disabled and replaced with manual scaling to prevent the introduction of additional limbs.
- **NTT:** Before injecting a bit-flip, we move the polynomial from evaluation space back to coefficient space using the inverse NTT (INTT). We flip the desired bit and transform the polynomial back to the evaluation space using NTT. After this hook, the pipeline continues normally.
- **Limitations of disabling NTT:** Since the NTT operates modulo q_0 , flipping bits beyond the bit-width of q_0 causes modular wraparound, which can alter the intended effect of the bit-flip and potentially lead to catastrophic decryption errors. To minimize distortion in the analysis, we set q_0 to the maximum value supported by the library—60 bits—ensuring that most bit-flips occur within the valid range and reducing unintended side effects from modular arithmetic.

Another difference is that in *OpenFHE*, the plaintext and the ciphertext live in the same ring. They both have polynomial coefficients of size q_0 , regardless of the Δ .

3) *Vanilla CKKS over Vanilla OpenFHE Validation:* To ensure that Vanilla *OpenFHE* mode faithfully replicates the behavior of *HEAAN* 1.0, we follow these validation steps:

- 1) Configure *OpenFHE* in vanilla mode (not using RNS and NTT) and set q and Δ to match *HEAAN*'s effective bit precision.
- 2) Restrict input values in *HEAAN* to real numbers, in line with *OpenFHE*'s plaintext constraints.
- 3) Compare L_2 norms and error statistics after identical bit-flips in both libraries.
- 4) Verify consistent sensitivity patterns across low- and high-order bit positions.

For more consistency and for better performance, we use *OpenFHE* in all our study. Internally we keep doing some of the experiments with *HEAAN* to still validate it.

4) *Internal Error Detection in OpenFHE:* *OpenFHE* includes an internal consistency check that estimates the standard deviation of the imaginary part of the decoded *plaintext*, designed to detect potential secret key leakage attacks. Flipping high-order bits at different stages of the homomorphic pipeline can result in substantial deviations, triggering this mechanism and aborting the decoding. To isolate the analysis of numerical resilience, we disable this mechanism.

This methodology enables controlled and reproducible exploration of both vanilla and optimized CKKS configurations, allowing for a rigorous assessment of the impact of single-bit faults at various stages of the homomorphic pipeline.

D. Experimental Procedure

The general workflow for the experiments is as follows. In *OpenFHE*, depending on the configuration, ciphertexts or plaintexts may be internally represented either in coefficient space or in the NTT (evaluation) domain. Since we inject faults at the polynomial level, we must ensure that the target object is in the coefficient space before injecting the bit-flip and, after injecting the fault, return it to its original domain.

- 1) Encode and, if applicable, encrypt the input vector using the selected library.
- 2) Apply the inverse NTT (INTT) to bring the object into coefficient space.
- 3) Flip a single bit within one coefficient (64-bit precision in *OpenFHE*; arbitrary-precision in *HEAAN*).
- 4) Reapply NTT to return to evaluation space.
- 5) Proceed with the homomorphic operation pipeline.
- 6) Decrypt and decode the result.
- 7) Compute evaluation metrics.

We repeat this process for every bit position in each coefficient, across both *plaintext* and *ciphertext* scenarios in separate experiments. To account for statistical variability, we repeat each experiment using multiple input seeds.

This setup enables direct comparisons between optimized and baseline implementations, allowing us to isolate the individual impact of each optimization technique on error resilience.

E. Experimental Environment

All experiments were executed on a dedicated workstation equipped with an Intel Core i7-11700 CPU (8 physical cores, 16 threads, 16 MB L3 cache, base 2.50 GHz) and 32 GB DDR4 RAM (dual channel, 3200 MHz). The operating system is Arch Linux (kernel `Linux 6.9.7-arch1-1`, distribution snapshot `257.5-1`). No concurrent user processes or virtualization layers were present during measurements.

We compiled both *OpenFHE* 1.3.0 and *HEAAN* 1.0 in release mode using `g++ 13.2.1` with flags `-O3 -march=native -DNDEBUG`. For *HEAAN*, *NTL* (*NTL* 11.5.1) and *GMP* (6.3.0) were linked dynamically; *OpenFHE* was built with its default backend (no GPU acceleration). ASLR remained enabled (default kernel setting).

but does not affect deterministic arithmetic outcomes. All randomness derives from fixed PRNG seeds (Section IV-F); the system entropy pool or hardware RNGs are not used directly.

CPU frequency scaling ran under the performance governor to minimize run-to-run variance. Each experiment was executed in a single process with logical core pinning (taskset) to reduce scheduling noise. We flushed OS file caches only for initial binary loads; no disk I/O occurs in the inner loops. Wall-clock timing (when collected) used `std::chrono::steady_clock`; we did not include startup warm-up in the reported aggregates. Thermal throttling was monitored via `intel_powergadget`; no throttling events were observed.

F. Input Vector Generation and PRNG Control

Our analysis is application-agnostic, employing input vectors of random real numbers drawn from a uniform distribution. To assess the sensitivity of the CKKS scheme, we sample inputs from various intervals whose boundaries are defined by powers of two.

Unless otherwise specified, input values are sampled as uniformly distributed real numbers within the interval 0 to 256, and represented in double-precision floating-point format. The bounded input range enables testing multiple Δ , allowing for a more comprehensive analysis of their impact on encoding and rounding errors. We analyze the trade-off between precision and noise growth by varying the scaling factor Δ across a wide range, ensuring it stays within the coefficient bounds detailed in Section II-B.

To evaluate stability impact of the seed variation, we repeat each experiment (i.e., each bit-flip) 2500 times. Each repetition involves 100 different seeds for the scheme PRNG and 25 for the input generator. These seed combinations are fixed and shared across all experiments, ensuring a fair comparison using equivalent input conditions. The resulting variability across repetitions is very low, indicating that this sampling strategy is sufficient for the aims of the study.

G. Parameter Selection

In order to ensure reasonable computation times given the number of seeds, we first studied the effect of ring dimension on bit-flip sensitivity patterns. This parameter has the greatest impact on computational performance: a larger N provides better security, but at the cost of increased computation. Because we observed that the bit-flip sensitivity patterns remained consistent across experiments with different values of N , we opted for smaller ring dimensions. This choice both improves performance and facilitates visualization: it is far easier to discern structure in the behavior of a small set of coefficients in a single plot than to interpret patterns spread across thousands simultaneously.

H. Evaluation Metrics

Given the original decrypted vector \mathbf{x} (without bit-flips) and the resulting vector \mathbf{y} after error injection and decryption, we quantify the deviation introduced by each bit-flip by two complementary evaluation metrics:

a) *Mean Squared Error (MSE)*: We define the element-wise error as:

$$\delta_i = y_i - x_i$$

and the MSE is computed as:

$$\text{MSE} = \sqrt{\frac{1}{k} \sum_{i=1}^k \delta_i^2}$$

b) *Element-wise Relative Error*: For each decrypted element, we compute the relative error:

$$\epsilon_i = \frac{|y_i - x_i|}{|x_i|}$$

V. EXPERIMENTAL RESULTS

This section presents the results obtained from injecting single bit-flips during the encryption stage of the CKKS scheme, as described in Sec. IV, in order to evaluate its resilience against induced faults.

We conducted experiments using both the *vanilla* and RNS modes of OpenFHE 1.3.0. Our decision to focus on the encryption stage stems from the theoretical results shown in Sec. III, which were also confirmed by our experiments. In particular, flipping a bit in the c_0 polynomial of a ciphertext immediately after encryption has the same effect as flipping the same bit in the plaintext either after encoding or after decryption. Therefore, in our analysis we inject bit-flips directly into the ciphertext, which allows us to present results for three equivalent cases — flipping a bit in the plaintext before encryption, in the c_0 polynomial of the ciphertext, or in the decrypted plaintext — as well as for the distinct case of flipping a bit in the c_1 polynomial of the ciphertext.

A. Vanilla CKKS

We first analyze the *vanilla* CKKS scheme using OpenFHE, i.e., without RNS or NTT optimizations.

1) *Evolution of the L_2 norm under Single Bit-Flips*: To evaluate its fault sensitivity, we systematically flipped one bit at a time in the ciphertexts generated during encryption, covering all bit positions in both c_0 and c_1 polynomials. After each injection, the modified ciphertext was decrypted, and the L_2 -norm of the difference with respect to the fault-free (golden) output was computed. This metric quantifies the magnitude of the decoding error associated with each bit position.

Figure 7 shows the resulting L_2 -norm distribution for all possible single-bit flips, highlighting which regions of the ciphertext are most sensitive to faults.

We observe that, for the first polynomial c_0 , the behavior follows the theoretical trend shown in Fig. 4: the least significant bits are more resilient to bit-flips, with the error magnitude growing exponentially up to the bit position corresponding to the size of the modulus q , after which it drops to zero.

A notable difference between HEAAN and OpenFHE in its *vanilla* mode is that, in the latter, coefficient $N/2$ of c_0 is not absolutely robust. This deviation arises because OpenFHE,

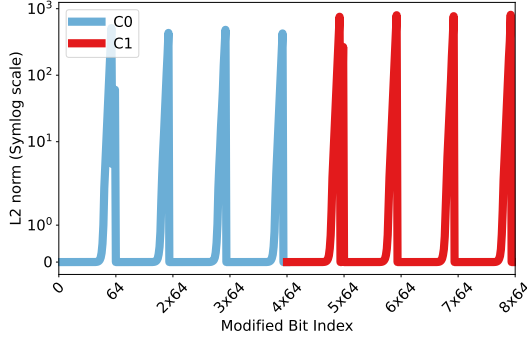


Fig. 7: Impact of a single-bit flip during encryption in OpenFHE without RNS or NTT. The horizontal axis indicates the position of the flipped bit within the ciphertext, while the vertical axis shows the resulting L_2 norm of the decoding error. Parameters: 60-bit modulus, scaling factor $\Delta = 2^{50}$, and ring dimension $N = 4$.

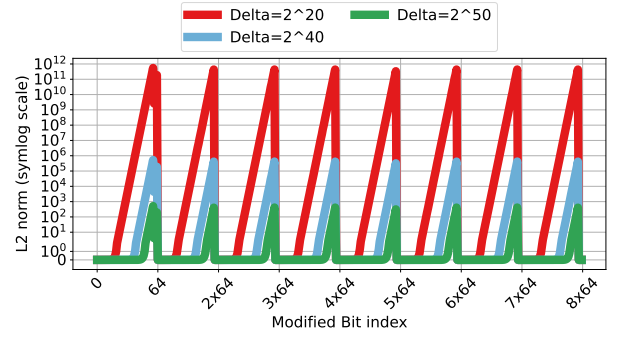


Fig. 8: Impact of a single-bit flip during encryption in OpenFHE without RNS or NTT. The x-axis indicates the bit position in ciphertext c_0 , while the y-axis shows the resulting L_2 norm of the decoding error on a symmetric log scale. Parameters: 60-bit modulus, scaling factors $\Delta = 2^{20}, 2^{30}, 2^{40}, 2^{50}$, and ring dimension $N = 8$.

during decoding, injects Gaussian noise into the coefficient vector prior to the DFT (a specialized FFT), perturbing both real and imaginary components as a countermeasure against key-recovery attacks.

The injected noise has a standard deviation proportional to the spread of the imaginary part of the pre-DFT vector, which—by the scheme’s properties—follows a Gaussian distribution. Flipping any bit in any coefficient, including $N/2$, alters this spread; higher-order bit flips have a stronger effect, increasing the overall noise variance and propagating it across all vector elements, thereby removing the theoretical robustness at $N/2$.

Disabling this noise injection in OpenFHE restores the expected behavior: coefficient $N/2$ of c_0 becomes robust to bit-flips. Since HEAAN 1.0 does not include this security noise, its experimental sensitivity matches the theoretical prediction exactly.

2) Impact of the Scaling Factor on Error Categorization:

One of the key parameters in the CKKS scheme is the scaling factor Δ . As analyzed in Sec. III, increasing Δ reduces the relative impact of a single-bit flip during encoding or encryption and also increases the proportion of bits that remain resilient to such faults.

To validate this behavior experimentally, we repeated the previous single-bit-flip analysis using four different scaling factors, namely $\Delta \in \{2^{20}, 2^{30}, 2^{40}, 2^{50}\}$. Figure 8 shows the L_2 norm of the decoding error for a bit-flip in the first ciphertext polynomial c_0 when running OpenFHE in simulated vanilla mode (i.e., with RNS and NTT disabled). For clarity, only results for c_0 are shown, since the behavior in this aspect for c_1 is analogous.

We observe that higher values of Δ yield lower L_2 norms after a bit-flip, indicating stronger attenuation of induced errors. Furthermore, the point at which the error norm begins its exponential growth shifts in alignment with the magnitude of Δ , confirming that larger scaling factors increase the number of error-resilient bit in each coefficient’s representation.

To provide a clearer interpretation, we then applied our second metric from Sec. IV, classifying each decryption outcome

into three categories based on the fraction of slots correctly recovered (relative error $< 1\%$):

- **Tail:** $> 99\%$ of slots correct
- **Middle:** $1\%–99\%$ of slots correct
- **Head:** $< 1\%$ of slots correct

For this experiment, we adopted a realistic setting with ring dimension $N = 2^{13} = 8192$ (i.e., 4096 encrypted slots). For each $\Delta \in \{2^{20}, 2^{40}, 2^{50}\}$ and each single-bit flip, we counted how many slots were correctly decrypted and assigned the result to one of the three categories. Figure 9 presents a histogram of the category frequencies for each scaling factor.

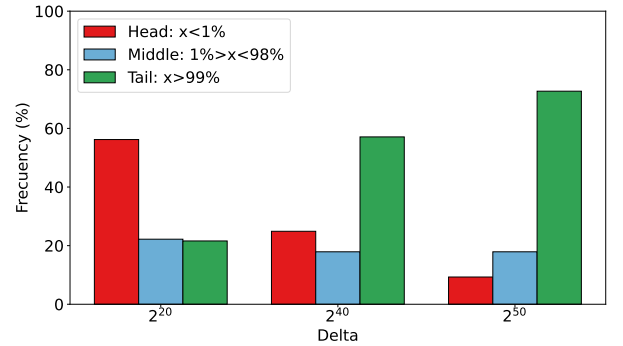


Fig. 9: Histogram of error-categorization outcomes for different scaling factors. Each group of bars corresponds to a specific Δ , showing the percentage of trials in the **Tail** ($> 99\%$ correct), **Middle** ($1\%–99\%$), and **Head** ($< 1\%$) categories, across all single-bit-flip experiments.

This distribution follows a bimodal ‘all-or-nothing’ pattern: in over 80% of the cases, either more than 99% or fewer than 1% of the slots are correctly decrypted. Importantly, as Δ increases, the frequency of **Tail** outcomes also increases, demonstrating that a larger scaling factor provides greater tolerance to noise, allowing the scheme to correctly decrypt more bits before significant error appears.

This behavior arises because a larger scaling factor increases the number of bits that are resilient to a bit-flip, resulting

in more cases falling into the tail outcome. Our analysis on Figure 8 also shows that the exponential growth of the L_2 norm after the first sensitive index (which closely tracks the scaling factor) is consistent across different values of Δ . Although we do not explicitly compute the L_2 norm threshold at which decryption completely fails, the observed consistency of the middle error category for each scaling factor demonstrates that the width of the transition interval—between full resilience and total failure—remains roughly constant for all Δ . This indicates that, regardless of the scaling factor, the number of “bits” representing this transition region does not change appreciably.

3) *Effect of the Input Value Representation Interval on Error Categorization:* We now analyze the impact of the effective input value representation interval. We fix $\Delta = 2^{20}$, which allows for a wider input range. Recall that the number of bits available for the integer part is approximately given by $q_0 - \Delta$. The effective representation interval refers to the ratio between the largest and smallest values that can be represented in fixed-point encoding. In our experiments, this interval is controlled indirectly by sampling input values uniformly between a minimum value and a maximum integer value, where the maximum is 2^{bits} .

In this case, with $q_0 = 60$ bit, the resulting effective input representation range is approximately 40 bit. Figure 10 shows histograms of the error category distributions for different input intervals, corresponding to the ranges $[2^9, 2^{10}]$, $[2^{19}, 2^{20}]$, and $[2^{29}, 2^{30}]$. We deliberately avoided using the full 40-bit range, since—as noted earlier—this is only an approximate upper bound, and near this limit, even unmodified input values may fail to decrypt correctly due to overflow.

In all experiments, we used the following parameters: ring dimension $N = 8192$, ciphertext modulus $q_0 = 60$ bit, and scaling factor $\Delta = 2^{20}$.

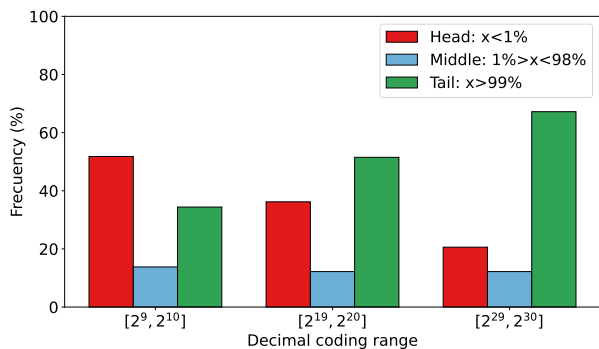


Fig. 10: Histogram showing the percentage of cases in which all elements were correctly decrypted (error $< 1\%$) and the percentage of cases in which all elements were incorrectly decrypted (error $> 1000\%$), for different values of dynamic range: 1, 10, 20, and 30 bits. Each bin corresponds to a specific dynamic range value, and the bars indicate how frequently each outcome occurred across bit-flip experiments.

We observe behavior similar to the impact of the scaling factor, as shown in Fig. 9. As the size of the input space increases, the percentage of correctly decrypted elements increases, while

the percentage of incorrectly decrypted elements decreases. Increasing the size of the input values, while keeping the scaling factor fixed, allows for the representation of values with greater relative precision compared to the existing noise.

This occurs because, for a fixed scaling factor, increasing the input value representation interval means that each value is represented with lower relative precision. Consequently, more values fall within the correct decryption threshold, leading to a higher proportion of correctly decrypted elements.

4) *Effect of reducing the number of encrypted elements:* As noted previously, CKKS can encode up to $N/2$ slots, where N is the ring degree (a power of two). When we encode fewer slots—still a power of two—we observe that additional coefficients remain unaffected by single-bit flips. Figure 11 shows results for $N = 16$ with only $N/4 = 4$ encrypted slots, allowing us to inspect a larger set of coefficients and evaluate their sensitivity.

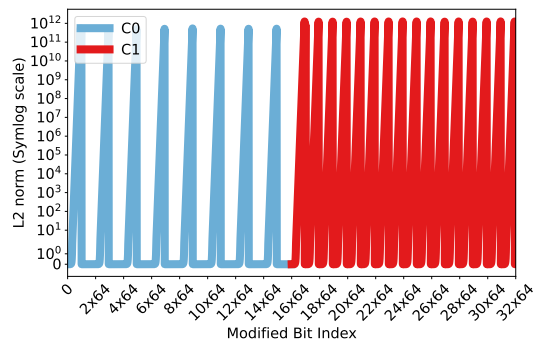


Fig. 11: Impact of a single-bit flip during encryption in OpenFHE without RNS or NTT. The horizontal axis indicates the bit position in the ciphertext, while the vertical axis shows the resulting L_2 norm of the decoding error. Parameters: 60-bit modulus, scaling factor $\Delta = 2^{20}$, ring dimension $N = 16$, and 4 encrypted slots.

The results reveal that odd-indexed coefficients of polynomial c_0 remain unchanged under bit-flips, whereas even-indexed coefficients exhibit the same sensitivity patterns observed earlier.

As explained in Sec. II, the ratio between the maximum number of slots ($N/2$) and the number actually used defines an interval—termed the *gap*—between the coefficients participating in the inverse transform. During the “special” FFT, only coefficients whose indices are multiples of this gap are considered and scaled in the input vector (see Sec. I for details).

Consequently, when encoding $N/2$ slots, all N coefficients of c_0 are sensitive to bit-flips; encoding $N/4$ slots reduces the number of sensitive coefficients of c_0 to $N/2$; and so on. In the case of c_1 , no matter the number of slots used, all coefficients are sensitive to bit changes.

B. Resilience under an intermediate RNS mode without NTT

We next conducted experimental campaigns to assess CKKS’s sensitivity when using only one of the numeric optimizations—either NTT or RNS. In both pure-NTT and

pure-RNS configurations, any single-bit flip caused decryption errors of unacceptable magnitude. As shown in our theoretical analysis, bit-flips under RNS produce errors several orders of magnitude larger than under NTT, while NTT alone still yields extremely large errors that preclude practical precision.

An interesting case emerges when CKKS is run with RNS only and the number of encrypted slots is halved or more. Figure 12 reports results for ring dimension $N = 16$ with only 4 encrypted slots (i.e., one power-of-two below the maximum), scaling factor $\Delta = 2^{20}$, and 8-bit input values.

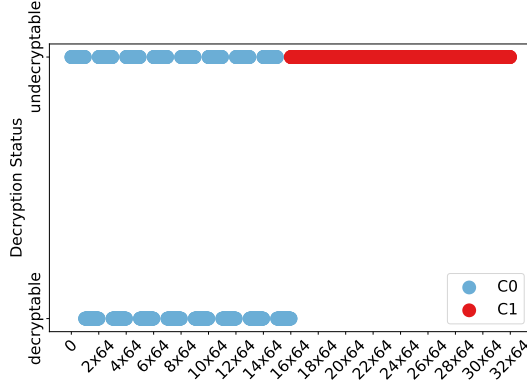


Fig. 12: Impact of a single-bit flip during encryption in OpenFHE without NTT but with two-limb RNS. The horizontal axis indicates the flipped bit position; the vertical axis denotes whether decoding succeeded ($< 1\%$ error) or failed ($> 1000\%$ error). Parameters: 60-bit modulus, $\Delta = 2^{20}$, $N = 16$, and 4 encrypted slots.

We observe that *odd*-indexed coefficients of c_0 remain fully robust: all their slots decrypt correctly with error below 1%. Any bit-flip in an *even*-indexed coefficient, however, causes decoding failures with errors exceeding 1000%. The number of sensitive coefficients exactly matches the “gap” analysis from Sec. V-A4.

Polynomial c_1 exhibits no robust bits at all: every bit-flip causes uniform decoding failure, so its error-categorization is flat and standard deviation is zero.

These results demonstrate that running CKKS with RNS only—together with a non-maximal but non-zero gap—can concentrate robustness on a subset of coefficients. Such a configuration suggests a trade-off between ring utilization and fault resilience. Future work may explore tailored RNS parameterizations to minimize sensitivity to bit-flips while preserving sufficient slot capacity, laying the groundwork for error-reduction strategies in homomorphic encryption schemes that balance precision and fault tolerance.

1) *MNIST Example*: To illustrate the practical impact of bit-flip resilience in CKKS, we consider a realistic input based on the MNIST dataset. Each image consists of $28 \times 28 = 784$ grayscale pixels, with integer values ranging from 0 to 255.

In order to encode 784 values using CKKS batching, we need a vector size that is a power of two and greater than or equal to 784; the smallest such size is $2^{10} = 1024$. Since CKKS requires a ring dimension N that is twice the batch size, we need $N \geq 2^{11} = 2048$.

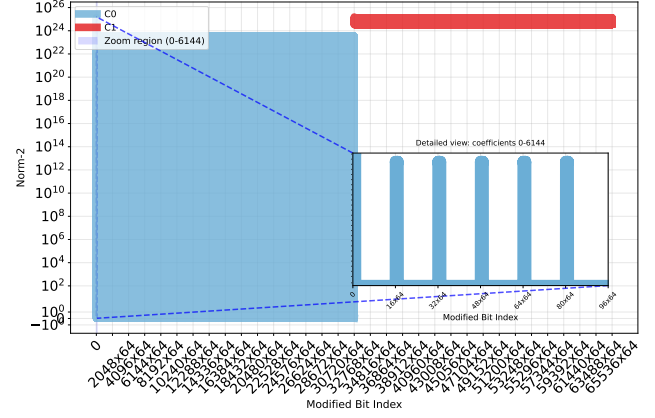


Fig. 13: Impact of a single-bit flip during encryption of MNIST images in OpenFHE with 3 RNS limbs without NTT. The horizontal axis indicates the position of the flipped bit within the ciphertext, while the vertical axis shows the resulting L2 norm of the decoding error. Parameters: 60-bit modulus, scaling factor $\Delta = 2^{20}$, and ring dimension $N = 2^{15}$.

However, to comply with standard security requirements, we select a ring dimension of $N = 2^{15}$, which provides a secure parameter set. This results in a large number of unused coefficients. Specifically, only the first 2^{11} slots of the plaintext or the c_0 polynomial of the ciphertext store actual image data, while the remaining $2^{15} - 2^{11}$ coefficients are unused.

As discussed in Sec. II-C, in this configuration the parameter $\text{gap} = \frac{N/2}{\text{batch size}} = \frac{2^{14}}{2^{10}} = 2^4 = 16$. Therefore, only $N/16 = 2^{15}/2^4 = 2^{11} = 2048$ coefficients in the c_0 polynomial will be affected by a bit-flip injected within the relevant slots. The remaining coefficients remain unaffected.

This means that over 93.75% of the encoded coefficients or the 46.87% of the ciphertext coefficients (because all c_1 coefficients remain sensitive) are inherently resilient to single-bit or multi-bit faults in this scenario.

Figure 13 shows results for $N = 2^{15}$ with only 2^{10} encrypted slots of MNIST images data base, a q -modulus of 60 bits, and a scaling factor of 2^{20} .

As expected, flipping any bit in the c_1 polynomial consistently produces an undecryptable result, whereas in c_0 only about one in every sixteen coefficients is sensitive to bit-flips.

However, this improvement comes at a substantial computational cost.

As we already explain in Sec. II, NTT-based multiplication enables fast polynomial product computations with a complexity of $\mathcal{O}(n \log n)$, where n is the ring dimension. When NTT is disabled, the underlying polynomial multiplication reverts to a naive or schoolbook approach with complexity $\mathcal{O}(n^2)$.

This quadratic cost affects all stages that involve polynomial multiplications, such as Encryption, decryption, ciphertext-ciphertext multiplication, relinearization, and others. As a result, homomorphic operations become orders of magnitude slower when operating in coefficient space without NTT.

Although we do not perform direct runtime benchmarking in this study, prior works such as [5] report performance slowdowns of approximately $10\times$ when switching from the

RNS+NTT-optimized scheme to the vanilla CKKS implementation.

In scenarios where RNS is used but NTT is disabled, the degradation is expected to be smaller, since RNS still reduces the cost of large-integer arithmetic by enabling parallel residue computations.

In practice, the exact slowdown depends on various factors, including the specific implementation, the chosen ring dimension, and the availability of hardware-level optimizations (e.g., SIMD instructions or parallel FFTs).

This highlights a fundamental trade-off between fault resilience and computational efficiency, which must be carefully balanced in real-world deployments.

C. Summary and Comparison

We provide a high-level comparison of the different CKKS configurations evaluated in this work. For each scenario, we highlight the key resilience pattern and any notable observations.

- **Vanilla CKKS:**
 - Least-significant bits exhibit robustness; error grows exponentially for higher bits.
 - Coefficient $N/2$ robust in HEAAN 1.0 but not in OpenFHE vanilla (due to Gaussian noise injection).
- **Varying Δ :**
 - Larger Δ delays the onset of exponential error growth to more significant bits.
 - $\Delta \geq 2^{30}$ yields **Tail** outcomes in over 80% of trials.
- **Effective Representation Range:**
 - Increasing integer-part range raises **Tail** frequency and reduces **Head** frequency.
 - Behavior parallels that of increasing Δ .
- **Reduced Slots:**
 - Encoding fewer slots reduces the number of sensitive coefficients in c_0 .
- **RNS without NTT:**
 - Some coefficients of c_0 remain robust; all flips in c_1 fail.
 - Demonstrates a “gap”-driven concentration of robustness when using RNS only.

This concise overview highlights how each parameter adjustment—from vanilla through optimized variants—modulates CKKS’s fault tolerance, guiding practical parameter selection under two-column constraints.

VI. CONCLUSIONS

This paper has presented a comprehensive evaluation of CKKS’s sensitivity to single-bit flips, emphasizing the influence of RNS and NTT optimizations on error resilience. While the vanilla CKKS implementation exhibits substantial innate tolerance to individual bit-flip faults, the optimized variants—with RNS or NTT enabled—display markedly increased vulnerability, potentially undermining the correctness of decrypted outputs.

Our findings indicate that, despite its performance drawbacks, vanilla CKKS offers a robustness advantage by minimizing the impact of isolated bit errors compared to its optimized counterparts. Furthermore, when employing large ring dimensions for security, encoding fewer slots (powers of two below the maximum) introduces redundancy that renders a subset of coefficients entirely insensitive to bit-flips. This “gap”-driven effect persists even in optimized configurations, highlighting a practical mechanism for enhancing resilience without altering core codec operations.

Overall, these results deepen our understanding of fault tolerance in homomorphic encryption schemes and provide actionable guidance for balancing throughput, security, and error resilience when selecting CKKS parameters.

a) *Future Work:* Promising directions include studying error tolerance in application-specific domains—such as deep neural networks for image processing, where limited accuracy loss is acceptable—and conducting a detailed investigation of error propagation under multiple concurrent bit-flips. Such analyses will further illuminate strategies for error mitigation in practical homomorphic computing scenarios.

ACKNOWLEDGMENTS

First, I would like to thank Pradip Bose, whose inspiration to explore fault tolerance in homomorphic encryption significantly shaped this work. I also appreciate the open-source homomorphic encryption community and the developers of the OpenFHE and SEAL libraries, whose tools and documentation greatly facilitated our experiments. In particular, I extend my gratitude to Ahmad Al Badawi for his help setting up OpenFHE correctly and for his clear explanations and references on CKKS encoding and decoding.

REFERENCES

- [1] R. L. Rivest, A. Shamir, and L. Adleman, “A method for obtaining digital signatures and public-key cryptosystems,” *Communications of the ACM*, vol. 21, no. 2, p. 120–126, Feb. 1978.
- [2] J. Ma, S.-A. Naas, S. Sigg, and X. Lyu, “Privacy-preserving federated learning based on multi-key homomorphic encryption,” *International Journal of Intelligent Systems*, vol. 37, no. 9, pp. 5880–5901, 2022.
- [3] M. Zhang, L. Wang, X. Zhang, Z. Liu, Y. Wang, and H. Bao, “Efficient clustering on encrypted data,” in *Applied Cryptography and Network Security*, C. Pöpper and L. Batina, Eds. Cham: Springer Nature Switzerland, 2024, pp. 213–236.
- [4] Y. Zhang, Y. Miao, X. Li, L. Wei, Z. Liu, K.-K. R. Choo, and R. H. Deng, “Efficient privacy-preserving federated learning with improved compressed sensing,” *IEEE Transactions on Industrial Informatics*, vol. 20, no. 3, pp. 3316–3326, 2024.
- [5] J. H. Cheon, K. Han, A. Kim, M. Kim, and Y. Song, “A full RNS variant of approximate homomorphic encryption,” in *Proceedings of the International Conference on Selected Areas in Cryptography (SAC)*, C. Cid and M. J. Jacobson Jr., Eds., vol. 11349. Cham: Springer International Publishing, 2019, pp. 347–368.
- [6] F. Sabath, *Classification of Electromagnetic Effects at System Level*. New York, NY: Springer New York, NY, 2010, pp. 325–333. [Online]. Available: https://doi.org/10.1007/978-0-387-77845-7_38
- [7] T. Kolditz, T. Kissinger, B. Schlegel, D. Habich, and W. Lehner, “Online bit flip detection for in-memory b-trees on unreliable hardware,” in *Proceedings of the Tenth International Workshop on Data Management on New Hardware*, ser. DaMoN ’14. New York, NY, USA: Association for Computing Machinery, 2014, pp. 1–9.
- [8] O. Mutlu and J. S. Kim, “Rowhammer: A retrospective,” *IEEE Transactions on Computer-Aided Design of Integrated Circuits and Systems*, vol. 39, no. 8, pp. 1555–1571, 2020.

- [9] K.-J. Li, Y.-Z. Xie, F. Zhang, and Y.-H. Chen, "Statistical inference of serial communication errors caused by repetitive electromagnetic disturbances," *IEEE Transactions on Electromagnetic Compatibility*, vol. 62, no. 4, pp. 1160–1168, 2020.
- [10] Z. Li, H. Menon, D. Maljovec, Y. Livnat, S. Liu, K. Mohror, P.-T. Bremer, and V. Pascucci, "Spotsdc: Revealing the silent data corruption propagation in high-performance computing systems," *IEEE Transactions on Visualization and Computer Graphics*, vol. 27, no. 10, pp. 3938–3952, 2020.
- [11] S. K. Höeffgen, S. Metzger, and M. Steffens, "Investigating the effects of cosmic rays on space electronics," *Frontiers in Physics*, vol. 8, p. 318, 2020.
- [12] H. Dixit, "Silent data corruptions at scale," in *Proceedings of the International Symposium on On-Line Testing and Robust System Design (IOLTS)*. Institute of Electrical and Electronics Engineers, Inc, 2023, pp. 1–2.
- [13] D. J. Bernstein, "The tangent fft," in *International Symposium of Applied Algebra, Algebraic Algorithms and Error-Correcting Codes (AAECC)*, S. Boztaş and H.-F. F. Lu, Eds. Berlin, Heidelberg: Springer Berlin Heidelberg, 2007, pp. 291–300.
- [14] —, *Fast multiplication and its applications*, ser. Mathematical Sciences Research Institute Publications. United Kingdom: Cambridge University Press, 2008, pp. 325–384. [Online]. Available: <https://library.slmath.org/books/Book44/files/10bern.pdf>
- [15] V. Lyubashevsky, C. Peikert, and O. Regev, "A toolkit for ring-lwe cryptography," in *Proceedings of the Annual International Conference on the theory and applications of cryptographic techniques (EUROCRYPT)*, vol. 7881. Berlin, Heidelberg: Springer, 2013, pp. 35–54.
- [16] A. Costache, B. R. Curtis, E. Hales, S. Murphy, T. Ogilvie, and R. Player, "On the precision loss in approximate homomorphic encryption," in *Proceedings of the International Conference on Selected Areas in Cryptography (SAC)*. Berlin, Heidelberg: Springer-Verlag, 2024, p. 325–345.
- [17] V. van der Leest, G.-J. Schrijen, H. Handschuh, and P. Tuyls, "Hardware intrinsic security from d flip-flops," in *Proceedings of the Fifth ACM Workshop on Scalable Trusted Computing*, ser. STC '10. New York, NY, USA: Association for Computing Machinery, Oct. 2010, p. 53–62.
- [18] J. F. Ziegler and W. A. Lanford, "Effect of cosmic rays on computer memories," *Science*, vol. 206, no. 4420, pp. 776–788, 1979.
- [19] P. V. A. Mohan, *Residue Number Systems: Theory and Applications*. Birkhäuser Chama, 2016.
- [20] A. A. Badawi, A. Alexandru, J. Bates, F. Bergamaschi, D. B. Cousins, S. Erabelli, N. Genise, S. Halevi, H. Hunt, A. Kim, Y. Lee, Z. Liu, D. Micciancio, C. Pascoe, Y. Polyakov, I. Quah, S. R.V., K. Rohloff, J. Saylor, D. Suponitsky, M. Triplett, V. Vaikuntanathan, and V. Zucca, "OpenFHE: Open-source fully homomorphic encryption library," *Cryptology ePrint Archive*, Paper 2022/915, 2022. [Online]. Available: <https://eprint.iacr.org/2022/915>